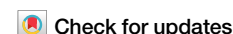# Mechanism of Cr(VI) removal by polyphenols-rich bacterial cellulose gel produced from fermented wine pomace

Check for updates

Zhi-yu Li [1] ✉, Jia-jia Dong[2], Fidelis Azi[3], Xue Feng[4], Zhi-wen Ge[4], Sha Yang[5], Yu-xia Sun[1], Xue-qiang Guan[1] & Ming-sheng Dong [4] ✉

Hexavalent chromium (Cr(VI)) is still a common contaminant in water. In this work, we studied the Cr(VI) adsorption by polyphenol-rich bacterial cellulose(BC) gel, synthesized by the Komagataeibacter rhaeticus K15 using wine pomace. The results showed that the equilibrium removal capacity was 473.09 ± 1.41 mg g^{-1} (dry weight). The quasi-second-order kinetics model and the Langmuir removal isotherm model was the most suitable for describing the Cr(VI) removal process. Toxic Cr(VI) was converted to the low toxic Cr(III) during the removal process via the reduction of Cr(VI) to Cr(III) by polyphenols released into the solution by the BC gel. The FTIR, XRD, XPS, SEM-EDX results indicated the physical adsorption on the surface of BC and the reduction reaction between polyphenol groups and Cr(VI) is the critical mechanism of Cr(VI) removal by BC. The finding of this study demonstrates that polyphenols-rich BC gel produced from wine pomace has a superior feature for future Cr(VI)-wastewater purification.

In the past decades, water pollution has become a global problem with the rapid development of industry and economy. Mining, cement and ceramics, battery manufacturing, leather tanning and plating, plastic production, and other industries that produced large amounts of industrial wastewater containing toxic heavy metals (lead, mercury, cadmium, chromium, etc.)[1]. These seriously threaten environmental safety and human health due to their non-degradability, carcinogenicity, and high toxicity[2–5]. There are two forms of chromium in wastewater: Cr(III) and Cr(VI)[6]. In the environment, chromium exists naturally as Cr(III), which is almost non-toxic and an important trace element essential for metabolizing lipids, glucose, and amino acids[7]. However, Cr(VI) was water-soluble, toxic, mutagenic and carcinogenic was deemed one of the most toxic heavy metal pollutants in water bodies[8]. Thus, the reduction of Cr(VI) to the less toxic Cr(III) is an effective strategy for the treatment of Cr(VI) water pollution. Cr (III) and Cr (VI) are interconvertible, and Cr (VI) can be reduced to Cr (III) by zero-valent nanoiron (nZVI)[9], FeS[10], biochar[11], and adsorbent materials rich in hydroxyl and amine groups[12], etc. At present, the main methods for Cr(VI) wastewater treatment were precipitation[13], electroplating[14], adsorption[15], ion exchange[16], membrane separation[17], photocatalytic reduction[18],

electrochemical condensation[19], etc. Among these methods, adsorption was the most widely used method for for removing Cr(VI) because of its simplicity, economy and environmental friendliness[20]. Although several researched products were used for water treatment, most were expensive, contribute to significant environmental pollution, and have not been applied to successfully treat large-scale wastewater successfully[21].Therefore, there was an urgent need to produce more green, environmentally friendly, and efficient water treatment materials to treat for the wastewater on a large scale. Degradable biomass materials can be considered as a good candidate for the real water treatment systems.

Bacterial cellulose (BC) is a renewable and environmentally friendly cellulose nanofiber produced through microbial fermentation[22,23]. BC's natural abundance, low cost, biocompatibility, 3D interconnected porous network, high porosity, abundant oxygen functional groups, and physico-chemical stability give them great potential for environmental remediation[22]. However, pure BC cannot remove heavy metal ions because it lacks active sites on its surface[24]. Lu, et al.[25] found the maximum removal capacity of BC on Cr(VI) was close to 15% (about 5.13 mg g^{-1}, dry basis). Although the scavenging ability of pure BC for heavy metal ions is poor due

[1]Shandong Academy of Grape/Shandong Engineering Technology Research Centre of viticulture and grape intensive processing/Winegrape and Wine Technological Innovation Center of Shandong Province, Jinan, Shandong 250100, China. [2]College of Pharmacy, Nanjing University of Chinese Medicine, Nanjing 210023, PR China. [3]Department of Chemical Engineering, Guangdong Technion-Israel Institute of Technology (GTIIT), Shantou, Guangdong 515063, China. [4]College of Food Science &Technology, Nanjing Agricultural University, Nanjing 210095, PR China. [5]Department of Food Technology, Safety and Health, Faculty of Bioscience Engineering, Ghent University, Coupure Links 653, 9000 Ghent, Belgium. ✉e-mail: lizhiyu1008@163.com; dongms@njau.edu.cn

Fig. 1 | Schematic diagram of polyphenol-rich BC gel membrane synthesis using wine pomace[29].
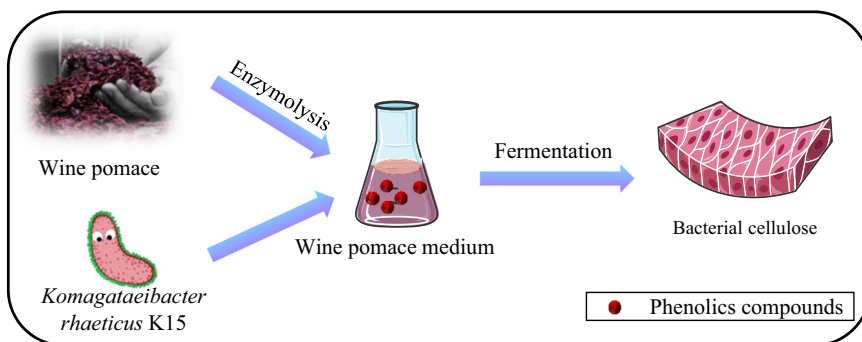
Fig. 2 | The effect of environmental factors on removal efficiency of Cr(VI). a The effect of initial pH value of Cr(VI) solution on removal efficiency of Cr(VI). **b** The concentration of initial Cr(VI) on Q_e of EW-BC. **c** The contact time on removal efficiency of EW-BC in different initial Cr(VI) concentration. **d** The coexisting ions on removal efficiency of Cr(VI). (Different lowercase letters in (**a**) and (**a**) indicated significant differences ($p < 0.05$). CK in (**d**) was control check, means that no coexisting ion was added to the solution except Cr(VI). "*", "***", and "****" indicate significant differences at $p < 0.05$, $p < 0.01$, and $p < 0.0001$ compared with CK, respectively. The Q_e (mg g^{-1}) in (**b**) and (**d**), Q_t (mg g^{-1}) in (**c**) were the removal capacity at removal equilibrium and the removal capacity at t (min) time, respectively. The error bars were standard deviation.
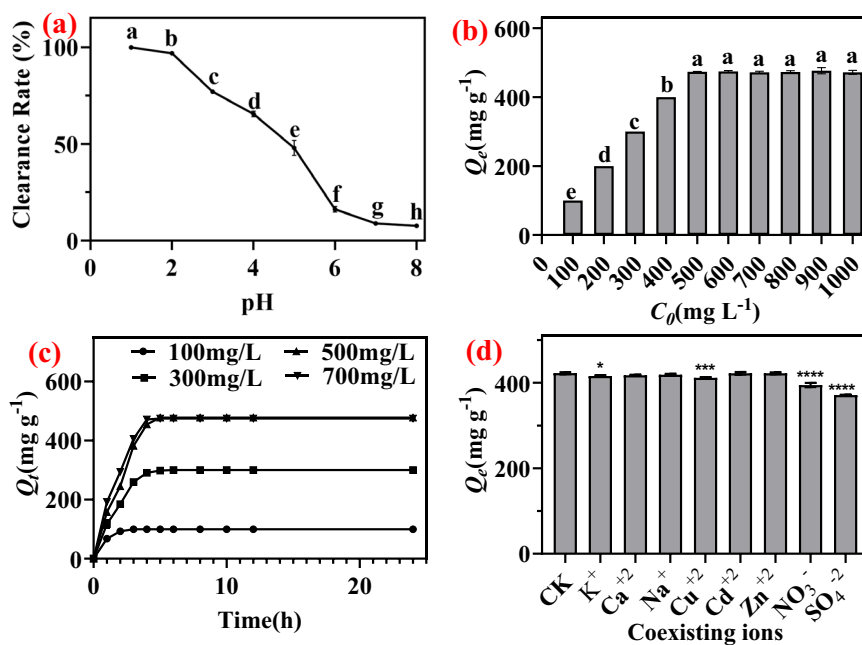
to the lack of active binding sites on the BC surface, modified BC loaded with various reductants showed a substantial reduction ability for Cr(VI)[25].

Polyphenol is a general term for a class of substances with multiphenolic chemical structures, which are common plant-derived bioactive substances widely found in fruits, tea, coffee and other foods[26]. They are potentially renewable, low-cost natural reductants for reducing Cr(VI)[27]. Chand et al. prepared a polyphenol-rich gel membrane by cross-linking with concentrated sulfuric acid and found a maximum Cr(VI) loading capacity of 1.91 mol kg^{-1} at pH = 4[28]. However, this method requires using concentrated sulfuric acid to extract cellulose, which is environmentally unfriendly.

In the previous study, we prepared a BC gel membrane using an environmental-friendly bio-conversion method, fermented by *Komagataeibacter rhaeticus* K15 using polyphenol-rich wine pomace[29]. Figure 1 summarized the preparation process of the BC gel membrane and diagrammatic drawing of its polyphenol loaded. The BC gel membrane in-situ bound grape polyphenols to the nanofiber, which loaded 90.62 ± 10.20 mg g^{-1} (Dry basis) insoluble-phenolics and 26.67 ± 0.28 mg g^{-1} (Dry basis) soluble-phenolics[29]. In addition, BC synthesized from wine pomace hydrolysate exhibited a slow release of phenolic compounds according our previous study[29]. Hence, considering the low cost and environmentally friendly synthesis of BC and the high loading of hexavalent chromium reducing agent, this study utilized this BC gel membrane for the removal of hexavalent chromium from wastewater. The removal capacity of polyphenol-rich BC gel membrane on Cr(VI) in water was investigated, and the removal conditions were optimized

to maximize its removal capacity. In addition, the mental removal mechanism of Cr(VI) by the modified BC films was also studied using SEM-EDS, XRD, FTIR, and XPS. This study aims to provide a sustainable and green material for heavy metal removal in wastewater treatment.

Results and discussion
Factors affecting the Cr(VI) removal process
The pH value of the Cr(VI) solution affected the functional group charge and the chemical morphology of Cr(VI)[30]. Figure 2a showed the clearance rate of Cr(VI) using EW-BC film on Cr(VI) solutions at different pH. As shown in the figure, there was a high Cr(VI) clearance rate at a low initial pH, and the clearance rate of EW-BC film on Cr(VI) was 99.95 ± 0.03% at initial pH = 1. The Cr(VI) clearance rate decreased gradually with the pH increase. In Cr(VI) solution with pH = 8, the clearance rate of BC film was only 7.72 ± 0.54%. The existing species of chromium ions in solution and the surface charge on EW-BC could explain the effect of initial pH on Cr(VI) adsorption onto EW-BC. The membrane zeta potential of BC and EW-BC was measured, as shown in Fig. 3. It was found that the point of zero charge (isoelectric point) occurred at around pH = 2.5, below which the BC and EW-BC were positively charged. Besides, the EW-BC had a higher zeta potential than BC at pH < 2.5, indicating that EW-BC had more positive charges at low pH. The Cr(VI) exists in an aqueous solution in the form of HCrO$_4^-$ under the condition of pH < 2, and the adsorption of the negative Cr(VI) species was easy to be adsorbed by the positive charges of hydroxyl H atom through electrostatic attraction under an acidic condition[30]. However,
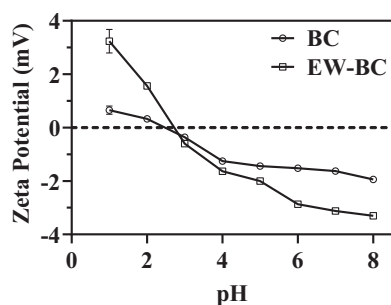
Fig. 3 | Zeta potential profiles for BC and EW-BC membrane at pH 1–8. The error bars were standard deviation.

the dominant form of Cr(VI) changed to a larger ionic size, $Cr_2O_7^{2-}$ gradually, with the pH increased, making it more challenging to diffuse in the solution so that it was resistant to the adsorption process[31]. It was reported that $HCrO_4^-$ could be adsorbed on the adsorbent through esterification reaction with polyphenol groups in phenolic compounds, and a high concentration of H^+ was conducive to the occurrence of this reaction, while the high concentration of OH^- inhibits the removal reaction[28]. Grape was rich in polyphenol compounds, and our previous studies confirmed these phenolic compounds could be combined in-situ with BC film[29]. The polyphenol groups of BC film under lower pH tended to have esterification reactions with Cr (VI) as described by Nakano et al.[32]. In addition, Chand et al. used grape waste gel rich in polyphenols for the adsorption of Cr (VI), which confirmed the oxo anions Cr (VI) was adsorbed on the adsorbent by an esterification reaction with functional groups of catechol at high H^+ concentrations in water[28]. However, the esterification reaction gradually slowed down or stopped with the increase of pH value. Based on above adsorption mechanisms, it suggested that an acidic condition facilitates the adsorption whereas an alkaline media will suppress the adsorption of Cr(VI), thus the BC film clearance rate of Cr (VI) declined with the increase of pH value. Industrial wastewater usually required several steps of treatment to achieve discharge standards, including heavy metal ion removal, acid and base neutralization, and physical settlement, etc. Therefore, the adsorption of Cr (VI) before the extreme pH being neutralized was a feasible measure. Hence, pH = 1 was used as the research premise in the following study.

To study the relationship between the removal capacity of EW-BC and the initial concentration of Cr(VI), the scavenging capacity of EW-BC on Cr(VI) was studied within the initial concentration range of 100–1000 mg L^{-1}, as shown in Fig. 2b. When the Cr(VI) concentration was 100-500 mg L^{-1}, EW-BC removal capacity increased with the increased Cr(VI) concentration. When Cr(VI) concentration was in the range of 100–400 mg L^{-1}, the clearance rate of EW-BC on Cr(VI) was 99.99%, while the removal rate of EW-BC on Cr(VI) at the initial concentration of 500 mg L^{-1} was 94.73%, and the equilibrium removal capacity was 473.09 ± 1.41 mg g^{-1} (dry weight). When the initial concentration was more significant 500 mg L^{-1}, the Cr(VI) equilibrium removal capacity of the EW-BC was stable at about 475 mg g^{-1} (dry weight), indicating that EW-BC had reached saturation removal capacity at this time. In addition, excessive Cr(VI) has no significant effect on the maximum removal capacity of EW-BC. Attractively, the EW-BC adsorbents exhibit a high Cr(VI) adsorption capacity, which was greater than many other adsorbents based on cellulose materials, such as hierarchical polydopamine-coated cellulose (205 mg g^{-1})[33], polyvinylimidazole modified cellulose (134 mg g^{-1})[34], amine-functionalized cellulose acetate beads impregnated aminated graphene oxide (410.21 mg g^{-1})[35], etc. These results indicated the potential of EW-BC to work efficiently in high Cr(VI) concentration environments due to historical Cr production operations and improper disposal of chromate slags[36].

Cr(VI) solutions with initial concentrations of 100, 300, 500, and 700 mg L^{-1} were selected to study the relationship between the removal capacity of EW-BC for Cr(VI) and contact time, as shown in Fig. 2c. As can be seen from the figure, the clearance rate of Cr(VI) on EW-BC decreased from fast to slow. The higher initial concentration of Cr(VI), the higher removal rate. A higher initial Cr(VI) concentration provided a relatively large mass transfer driving force, which was conducive to overcoming the resistance of Cr(VI) ions from the solution phase to the interior of EW-BC[37]. It can be seen from Fig. 2b that the maximum Q_t of these two groups was 99.98 ± 0.03 mg g^{-1} and 299.97 ± 0.02 mg g^{-1} when the initial Cr(VI) concentration was 100 and 300 mg L^{-1}, respectively. Although the adsorption rate was less than 100% after equilibrium removal at these two initial concentration conditions, the concentration of residual Cr(VI) in the solution was lower than the 0.05 mg L^{-1} required by the World Health Organization set the permissible limit for drinking water. No desorption occurred after continuous detection for 24 h, indicating that the EW-BC could be used as a potential wastewater treatment material. When the initial Cr(VI) concentration was 500 mg L^{-1} and 700 mg L^{-1}, the EW-BC rapidly adsorbed Cr(VI) within 4 h. The removal rate decreases and gradually reaches stability after 4–5 h. The change in removal rate from fast to slow was mainly due to the change in the number of adsorption sites. Initially, The EW-BC's irregular 3D reticular fibers initially had many adsorption sites on which Cr(VI) was rapidly absorbed. As the removal process progresses, the empty adsorption sites of EW-BC gradually decreas, and the removal rate slows down until equilibrium is reached. In addition, the adsorption sites of EW-BC tended to be saturated due to high concentration and excess Cr(VI), so the adsorption gradually stopped and reached equilibrium after 6 h. This result was consistent with the adsorption characteristics of BC-based heavy metal sorbents reported in the literature, which was mainly related to the characteristics of BC[38,39].

There were cations such as K^+, Ca^{2+}, Na^+, Cu^{2+}, Cd^{2+}, Zn^{2+} and anions such as NO_3^- and SO_4^{2-} in tanning, paint, mining and chrome plating industrial wastewater except for Cr(VI), which will affect each other in the treatment of heavy metal ions in wastewater[40]. The existence of anions in an aqueous solution could compete with Cr(VI) for the same adsorption site of EW-BC, and cations could even combine with Cr(VI),which sometimes inhibited the removal of Cr(VI)[41]. Based on the above theories, the effect of coexisting ions of cations K^+, Ca^{2+}, Na^+, Cu^{2+}, Cd^{2+}, Zn^{2+}, as well as anions NO_3^- and SO_4^{2-} on the removal of Cr(VI) by EW-BC was studied, as shown in Fig. 2d. Compared to the control, the ions in the solution had different degrees of adverse effects on the removal of Cr(VI) by EW-BC. For cations, the addition of Ca^{2+}, Na^+, Cd^{2+}, Zn^{2+} and other divalent cations in the solution had a relatively small effect on the removal of Cr(VI) by the EW-BC, and the statistics showed no significant difference in the equilibrium adsorption capacity of EW -BC compared with CK. The coexistence of K^+ and Cr(VI) had a relatively high effect on the adsorption performance of EW-BC, resulting in a significant difference. The coexistence of Cu^{2+} and Cr(VI) substantially influenced the removal performance of EW-BC, which might be because Cu^{2+} and phenolic substances can form complexes and thus produce competitive adsorption with Cr(VI)[42]. Compared with cations, anions had a more significant effect on the removal of Cr(VI) by EW-BC, and the addition of NO_3^- and SO_4^{2-} significantly reduced the equilibrium removal capacity of Cr(VI) by EW-BC, showing a statistically significant difference. Both NO_3^- and SO_4^{2-} in the solution had negative charges, and these anions will produce competitive inhibition with $HCrO_4^-$ with the same negative charge and react with the positive charge on the surface of EW-BC, thus reducing the adsorption effect of the adsorbent, which was consistent with the results reported in literature[41,43].

Desorption experiment

Figure 4 showed the desorption of EW-BC film in deionized water with different pH values after Cr(VI) was adsorbed and balanced. As can be seen from the figure, different pH has little influence on its desorption. No Cr(VI) was detected after 24 h of constant temperature shaker desorption under different pH conditions. However, the concentration of Cr(III) in the desorption solution was 44.21–46.27 mg L^{-1}, which might be due to the exchange of Cr(III) solution in EW-BC film with water in the environment, and Cr(III) flows into the desorption solution.
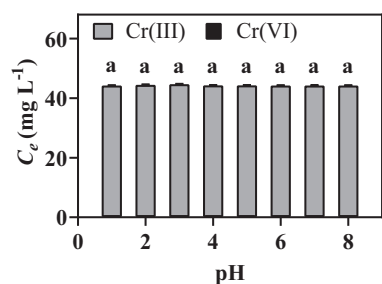
Fig. 4 | The desorption of EW-BC after Cr(VI) adsorption in deionized water with pH 1–8. The same lowercase letters indicated no significant differences ($p < 0.05$). The error bars were standard deviation.

Removal kinetics

Removal kinetics is one of the important contents of adsorbent research. These empirical or semi-empirical models play a crucial role in evaluating and verifying the effectiveness of removal experiments. Commonly used removal kinetics models mainly include quasi-second-order (PSO), quasi-first-order (PFO), intra-particle diffusion (IPD), elovich equation (EL), bangham equation (BNG), Weber-Morris intra-particle diffusion (WMIPD), etc., which correspond to different physical properties and reaction states respectively[44]. In this study, quasi-first-order kinetic and quasi-second-order kinetic models were used to describe the removal rule of the EW-BC on four different Cr(VI) concentrations because they are more suitable to describe the reaction between solid and liquid[45]. The removal data fitting results were shown in Table 1 and Fig. 5a.

Quasi-first-order kinetic models were used to describe the Cr(VI) removal process, mainly to describe the relationship between target ions and the number of effective removal sites[46]. The quasi-first-order kinetic model showed that during the reaction time, the removal rate was related to the available removal capacity, and the removal rate was appropriately dependent on the expression of concentration difference but not significantly reliant on the volume concentration of solute in solution[47]. In this study, the correlation coefficient R^2 after quasi-first-order kinetic model fitting was between 0.84954 and 0.97763. The quasi-second-order kinetic model was established in the 1980s after the quasi-first-order kinetics proposal, mainly used to describe the chemisorption relationship between adsorbent and target ion[48]. The correlation coefficient R^2 was between 0.97210 and 0.99836 after fitting with the quasi-second-order dynamics model. These two kinetic models were closely related to the relationship between the maximum removal capacity of the adsorbent and the first-order target ion concentration. The quasi-second-order kinetic model with a higher R^2 value was more suitable for describing the removal of Cr(VI) by EW-BC, indicating that chemical reaction had a more significant influence on the removal of Cr(VI) by EW-BC.

Removal isotherm

Removal isotherms reveal the removal mechanism and the interaction between adsorbents and adsorbents. In this study, Langmuir and Freundlich removal isotherm models were used to simulate the removal of Cr(VI) on EW-BC, as shown in Table 2 and Fig. 5b.

Langmuir's model was simple and intuitive, and the model calculation was very convenient. In this model, it was assumed that there were a limited number of binding sites on the surface of the adsorbent, each of which could be free or bound to the adsorbed molecule. The Langmuir model was used to simulate the removal of Cr(VI) on EW-BC. The results showed that the predicted maximum removal capacity was 483.78 mg g^{-1}, close to the actual experimental result. In this study, the K_L value of Langmuir was 0.59, within the range of 0−1, indicating that the removal of Cr(VI) by EW-BC could be deemed preferential adsorption[38]. The R^2 of the Langmuir removal isotherm was significantly higher than that of Freundlich, indicating that the Langmuir model was more suitable for describing EW-BC adsorption of Cr(VI).

Characterization of EW-BC before and after Cr(VI) removal

Figure 6a showed the FTIR spectra of EW-BC film before and after Cr(VI) adsorption at pH = 1. As can be seen from the figure, the strong absorption peak at 3345 cm^{-1} was associated with O-H stretching, the absorption peak at 2900 cm^{-1} was associated with C-H stretching, and the C-O-H of 1,4-β-glucoside was antisymmetry stretching at 1160 cm^{-1} [49]. The antisymmetric antiphase loop of β-glycosidic bonds between glucose units is stretched near 900 cm^{-1} [50]. In addition, the absorption peaks related to O-H folding were around 1360 cm^{-1}, 1280 cm^{-1}, and 1205 cm^{-1}, while the absorption peaks around 1430 cm^{-1} and 1335 cm^{-1} were related to bending in the O-H plane[17]. The peaks near 1108 cm^{-1}, 1050 cm^{-1}, and 1031 cm^{-1} were all related to C-O bending[46]. The above characteristic peaks related to cellulose structure did not change significantly before and after removal. In addition, the wide peak at 1242 cm^{-1} was related to phenolic groups in wine pomace[51].

Notably, extra absorption peaks appear near 804 cm^{-1} and 945 cm^{-1} after EW-BC absorbed Cr(VI). According to previous reports[30,38], these two peaks were related to Cr(III)-OH and Cr(VI)-O, respectively. The results showed that there were two valence states of Cr(III) and Cr(VI) after the removal of Cr(VI) by EW-BC film, indicating there were two processes of Cr(VI) removal and Cr(III) reduction in the contact process of BC to Cr(VI). The results were also confirmed by XPS and XRD (See below).

The XRD was used to characterize the crystal structure and physical properties of EW-BC film after Cr(VI) adsorption, as shown in Fig. 6b. The typical diffraction peaks of type-I cellulose near 14.7 °, 16.5 °, and 22.6 ° did not change significantly, indicating that adsorption of Cr(VI) did not change the structure of cellulose[52]. It is noteworthy that after Cr(VI) adsorption, the EW-BC exhibited strong 2θ diffraction peaks located at nearly 27° and two weak 2θ diffraction peaks located at near 35° and 42.5°, respectively, which was ascribed to Cr$_2$O$_3$ according to the reported literature[53,54]. In addition, the Jade 6.5 software was used for comparative analysis, and it was found that the most matched substance was Cr$_2$O$_3$, which was in good agreement with the reported literature[55,56]. These results indicated that Cr(III) reduction reaction occurred during the removal of Cr(VI) by EW-BC. On the other hand, no diffraction peak matching Cr(VI) related compounds were found in XRD results, indicating that the adsorption process of BC on Cr(VI) also exists. These results indicated that removing Cr(VI) by EW-BC was a simultaneous chemical reaction and physical removal process.

To further study the removal mechanism of EW-BC on Cr(VI), XPS analysis was performed on EW-BC samples before and after Cr(VI) adsorption, which was shown in Fig. 6c about the full spectra of XPS. The main elements of EW-BC before and after Cr(VI) adsorption were C, O, and N. The binding energy of C 1 s was around 285 eV, O 1 s was around 532 eV, and N 1 s was around 400 eV. It was worth noting that the full spectrum of EW-BC adsorbed Cr(VI) showed extra characteristic peak at 576.9 eV and 586.7 eV, which corresponded to Cr(III)-OH and Cr(VI)-O, respectively, not only in good agreement with the reported literature and by Thermo Avantage software analysis[30]. Moreover, these results was consistent with the above FTIR and XRD results, which indicated that the Cr(III) reduction reaction occurred during the removal of Cr(VI) by EW-BC. The removal of Cr(VI) by EW-BC involved both physical removal and chemical reaction. In addition, the peak intensities of C 1 s and O 1 s in the full spectrum of

Table 1 | The kinetic model parameters of Cr(VI) removal by EW-BC

Initial Cr(VI) concentration (mg/L)	Quasi-first-order dynamics model		Quasi-second-order dynamics model	
	K$_1$ (min^{-1})	R^2	K$_2$ (g/mg·min)	R^2
100	0.02237	0.97763	1.16939	0.99836
300	0.00165	0.84954	0.54357	0.98569
500	0.00103	0.92893	0.45636	0.97210
700	0.00142	0.94569	0.55349	0.98397

Fig. 5 | The adsorption model of Cr(VI) removal by EW-BC. a The quasi-first-order kinetic model and quasi-second-order kinetic model of Cr(VI) removal by EW-BC in initial Cr(VI) concentration of 100, 300, 500, and 700 mg L^{-1} respectively. **b** The Langmuir and Freundlich isotherm parameters for Cr(VI) removal by EW-BC. The Q_e (mg g^{-1}) were the removal capacity at removal equilibrium.
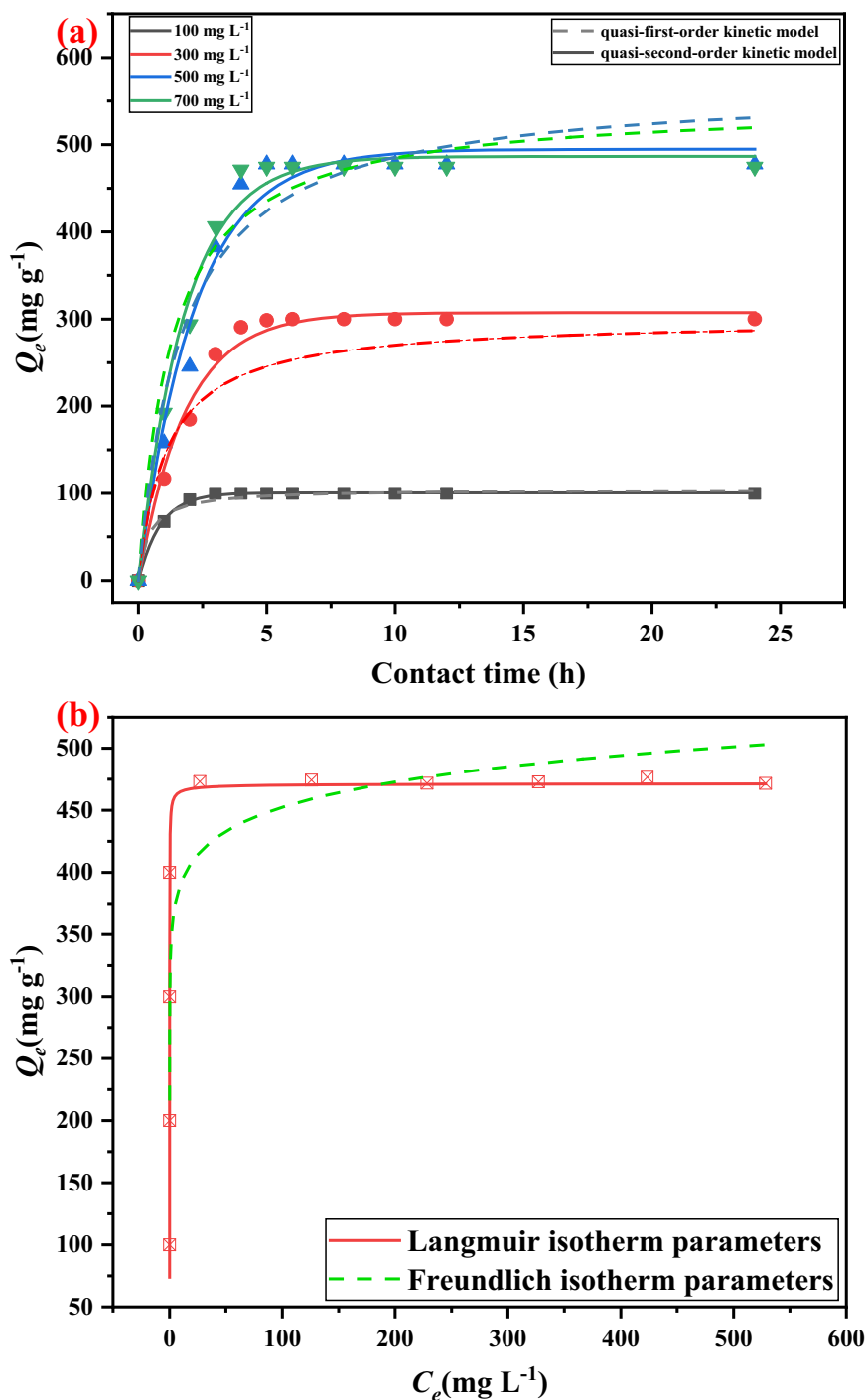
EW-BC after Cr(VI) removal were significantly enhanced, which might result in an oxidation reaction with Cr(VI) adsorbed by adsorbent, resulting in the formation of oxygen-containing groups.
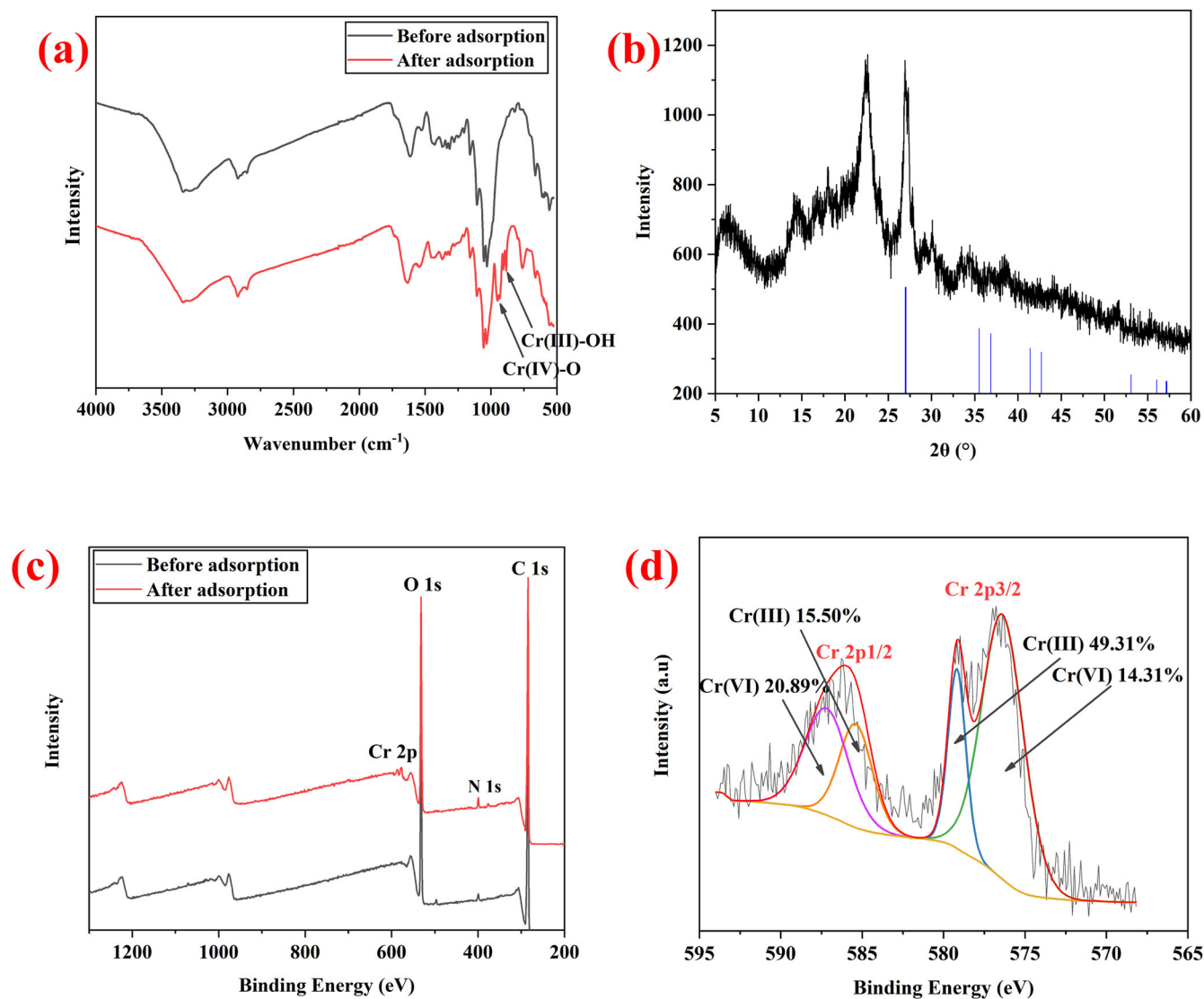
To further analyze EW-BC's changes in the Cr(VI) removal process, the high-resolution Cr2p spectrum in the XPS spectrum was peak-divided, and the results were shown in Fig. 6d. In the removal spectra, extra peaks

appeared at 586.4 eV and 577.0 eV, respectively, characteristic peaks of Cr 2p1/2 and Cr 2p3/2. Cr 2p3/2 was the distinct absorption peak of Cr(III)-OH and Cr(VI)-O at 577.0 eV and 579.0 eV, respectively.

In addition, the C 1 s, O 1 s, and N 1 s high-resolution spectra of EW-BC before and after removal were analyzed, respectively, as shown in Fig. 7. There was no significant change in the morphology of element C in the C 1 s spectrum before and after removal according to Fig. 7a. Still, the C-C content increased from 63.04% to 71.09% after removal, and the C-O content decreased from 26.71% to 19.29%, suggesting that some C-OH might contribute electrons and be oxidized during the removal process. According to Fig. 7b, the O 1 S profile changed greatly before and after removal, and the characteristic peaks corresponding to Cr(OH)$_3$ and Cr$_2$O$_7$$^{2-}$ appear at 531.0 eV and 529.9 eV, respectively, after removal. This result proved the removal and reduced Cr(VI) by EW-BC. Meanwhile, Fig. 7c showed the

Table 2 | The Langmuir and Freundlich isotherm parameters for Cr(VI) removal by EW-BC

(Q$_e$)$_{exp}$ (mg/g)	Langmuir			Freundlich		
	Q$_m$ (mg/g)	K$_L$	R^2	1/n	K$_F$	R^2
476.60	483.78	0.59	0.9299	0.064	337.41	0.7798

Fig. 6 | The characterization of EW-BC before and after Cr(VI) removal. a The FTIR spectra of EW-BC before and after Cr(VI) removal. **b** The XRD spectra of EW-BC after Cr(VI) removal. **c** The XPS spectra of EW-BC before and after Cr(VI) removal. **d** The Cr2p spectra of EW-BC after Cr(VI) removal.

morphology of the N element in the N 1 s map changed little after Cr(VI) removal.
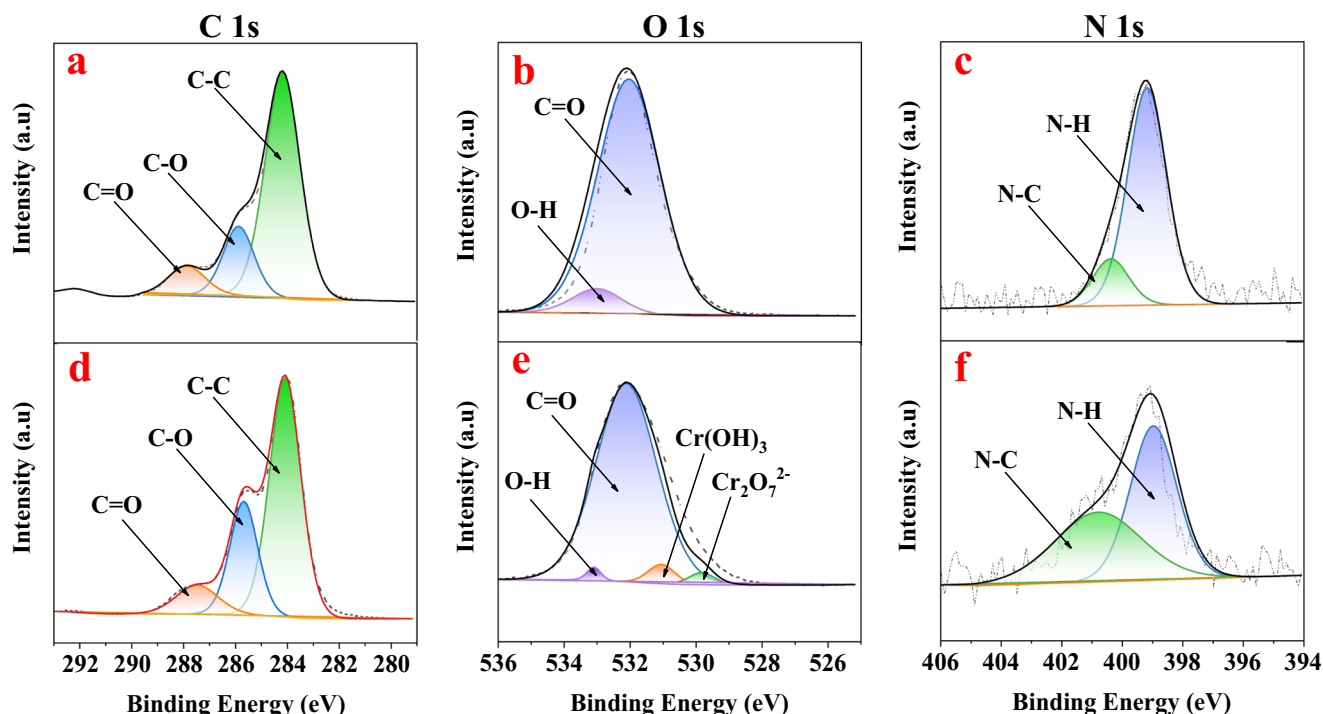
SEM-EDX was used to characterize EW-BC before and after Cr(VI) removal, and the results are shown in Fig. 8. It can be seen from the SEM figure that there was no significant difference ($p > 0.05$) in BC fiber structure before and after removal, and there were block shadows among the fibers, which might be due to the aggregation of polyphenols caused by the BC film being shaken violently in a 30 °C shaker. The EDX analysis showed that two strong peaks about Cr at 0.6 keV and 5.4 keV and one weak peak at 6.0 keV in the adsorbed EW-BC. In addition, the intensity of the C peak at 0.15 keV decreased obviously after removal.

Three different points were randomly selected from the SEM figure to further study the removal mechanism for quantitative analysis of C, O, N, and Cr elements, as shown in Table 3. After the removal of Cr(VI) on BC, the content of the C element decreased, while the concentration of the O element increased slightly, and the corresponding C/O ratio decreased. The increase of O element content might be due to the removal of chromium anions with oxygen atoms. At the same time, the decrease in the C/O ratio indicates that some C-OH may contribute electrons and oxidize during Cr(VI) reduction. In addition, the content of Cr in the adsorbed BC was $29.31 \pm 2.83\%$, which indicated that EW-BC could effectively remove Cr(VI).
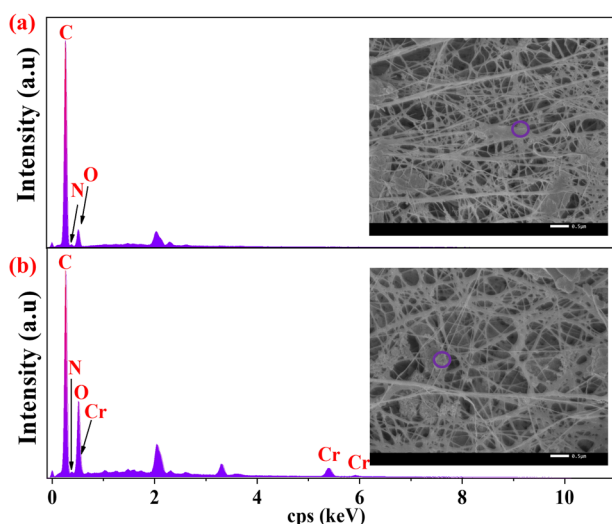
Removal mechanism of Cr(VI) by EW-BC

Cr(VI) removal was generally accompanied by several processes[30]. In order to understand the removal of Cr(VI) by EW-BC better, the optimal removal pH of Cr(VI) was selected according to the above research results, and the variation rules of Cr with different valence states in the process of EW-BC removal of Cr(VI) were studied, as shown in Fig. 9. When the initial Cr(VI) concentration was 500 mg L^{-1}, the Cr(VI) in the solution decreased gradually after adding EW-BC and reached equilibrium at 5 h. The total Cr content in the solution decreased progressively and reached equilibrium after 6 h. Initially, no Cr(III) was detected in the solution, but with increased removal, the content of Cr(III) in the solution gradually increased. The previous report also found the Cr(VI) removal was attributed to the gradual conversion of Cr(III) in the solution[30]. Therefore, it was speculated here that the conversion of Cr(VI) to Cr(III) in the solution was caused by the reaction of the loaded polyphenols in EW-BC with Cr(VI) and released into the solution. Cr(III) was an important trace element essential for the metabolism of lipids, glucose, and amino acids and is almost non-toxic[7].

Lu, et al.[25] showed that the original BC film had slight removal on Cr(VI) under the condition of pH < 1.5, and the maximum removal capacity was 8.5 mg g^{-1} (dry base). Shi, et al.[30] used lignin-modified BC to adsorb Cr(VI), with a maximum removal capacity of 898.2 mg g^{-1}. Through studying the removal mechanism, it was found that the removal of Cr(VI)

Fig. 7 | The high-resolution spectra of EW-BC before and after Cr(VI) removal. The C 1 s (**a**), O 1 s (**b**), and N 1 s (**c**) high-resolution spectra of EW-BC before Cr(VI) removal and the C 1 s (**d**), O 1 s (**e**), and N 1 s (**f**) high-resolution spectra of EW-BC after Cr(VI) removal.
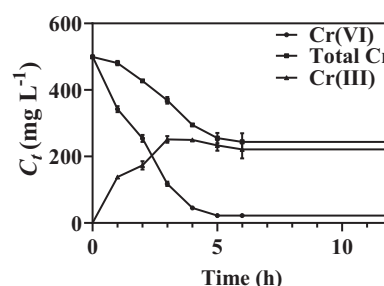

Fig. 8 | The SEM-EDX of EW-BC before and after Cr(VI) removal. a Before Cr(VI) removal. **b** After Cr(VI) removal. The scale bars represent 0.5 μm.

Table 3 | The changes of elements before and after Cr(VI) were adsorbed by BC

Element	Before the removal (wt %)	After the removal (wt %)
C	82.52 ± 3.78	51.86 ± 0.89
O	15.34 ± 2.23	18.09 ± 2.93
N	2.13 ± 1.93	0.74 ± 0.78
Cr	0	29.31 ± 2.83

Fig. 9 | The variation rules with time of Cr with different valence states in the process of Cr(VI) removal by EW-BC. The C_t (mg L^{-1}) was the concentration of different valence states chromium. The error bars were standard deviation.

by lignin-modified BC involved several processes, such as electrostatic attraction, ion exchange, complexation and partial reduction. Liu, et al.[57] showed that epicatechin gallate (EGCG) and Cr(VI) can react quickly and generate EGCG quinones under low pH conditions. In addition, Chen, et al.[58] confirmed that gallic acid could reduce Cr(VI) to Cr(III), and the reaction rate constant increased significantly with the decrease of pH value and the increase in temperature.

According to our previous study[29], the contents of water-soluble monomers such as catechin, epicatechin, and gallic acid in the medium from wine pomace were relatively high. These phenolic substances were in situ bound to EW-BC during fermentation and could reduce Cr(VI) to Cr(III) in the process of Cr(VI) removal. Meanwhile, according to the research results of Lu, et al.[25], BC can also absorb part of Cr(VI) due to its

electrostatic removal. In addition, the EW-BC film contains polyphenols according to our previous study[46]. The polyphenols released into the solution during the removal process also reduce Cr(VI) in the solution, culminating in the gradual increase in the solution's Cr(III) content. Summarily, the present data indicated that the Cr(VI) reduction mechanism by EW-BC was the reduction of Cr(VI) to Cr(III) by soluble-phenolics of EW-BC and polyphenols released into the solution from EW-BC. In addition, a portion of Cr(VI) and Cr(III) was adsorbed by BC (Fig. 10). The Cr(VI) reduced to Cr(III) by the EW-BC

Fig. 10 | The schematic diagram of removal process of Cr(VI) by EW-BC.

polyphenols were subsequently bound to BC fiber and removed from the solution.

In brief, this work demonstrated the detailed construction of potency for the Cr6+ removal using a polyphenol-rich bacterial cellulose gel membrane, which was synthesized in-situ by the *Komagataeibacter rhaeticus* K15 from wine pomace. The pH significantly influenced the removal capacity of the BC gel membrane, and the removal capacity increased with the increase of the Cr(VI) initial concentration. Moreover, the kinetic data agreed with quasi-second-order, while the obtained data from isotherms pointed out that Langmuir models were the most convenient models for describing the adsorption process. Various characterization tools were stimulated to emphasize the removal mechanism, indicating that physical removal on the surface of BC and the reduction reaction between polyphenol groups and Cr(VI) is the critical mechanism of Cr(VI) removal by BC. This work could open a horizon in polyphenols-rich BC film produced from wine pomace in the industrial treatment of heavy metals-containing wastewater.

Methods
Materials
All reagents were analytical reagents. Potassium dichromate, acetone, potassium chloride, calcium chloride, sodium chloride, copper chloride, zinc chloride, sodium sulfate, concentrated sulfuric acid, and sodium hydroxide were all purchased from Nanjing Chemical Reagent Co., Ltd., China. Diphenyl carbazide was purchased from Shanghai Yuan ye Bio-Technology Co., Ltd., China. Cadmium chloride, sodium nitrate, and concentrated hydrochloric acid were all purchased from Sinopharm Chemical Reagent Co., Ltd., China. Pectinase (8000 U mL^{-1}) and cellulase (60,000 U mL^{-1}) were purchased from Cangzhou Xiasheng Biotech Co. Ltd., China.

In situ synthesis of polyphenol-modified BC gel membrane
The preparation of BC gel membrane was obtained in the fermentation of enzymatic hydrolysate of wine pomace, according to our previous studies[17,29]. 500 g of wine pomace was mixed with 1000 mL acetate buffer (100 mmol L^{-1}, pH 5.50) and homogenized for 10 min using an agitator (Joyoung, L6, China). Then, the homogenate was hydrolyzed using commercial enzymes with pectinase and cellulase. The coverage of pectinase and cellulase were 500 U g^{-1} and 1500 U g^{1} (dry basis wine pomace), respectively. The hydrolysis was performed with 150 rpm shaking at 55 °C for 12 h. Afterward, the enzymatic hydrolysate of wine pomace was centrifuged, and the supernatants were obtained. Finally, the enzymatic hydrolysate was fermented using *Komagataeibacter rhaeticus* K15 at 30 °C for 10 d under static conditions.

After that, the BC gel membrane was collected and then rinsed with ultrapure water to wipe off the medium of the BC surface. Then, the BC gel membrane was soaked with 0.05 mol L^{-1} NaOH for 0.5 h at 80 °C to dislodge bacterial cells inside BC. Subsequently, rinsed BC with flowing ultrapure water until the pH of BC surface was neutral. According to the previous study[29], the purified BC yield from enzymatic hydrolysate of wine pomace was 4.28 ± 0.21 g L^{-1} (dry basis), and the cellulose purity was $90.96 \pm 2.15\%$. In addition, the BC film from enzymatic hydrolysate of wine pomace was named EW-BC, which showed the ability to load grape polyphenols according to our pervious study[29].

Cr(VI) removal capacity calculation
Cr(VI) removal rate $R\%$ was calculated according to Formula 2−1:

$$R\% = \frac{C_0 - C_e}{C_0 \times 100} \tag{1}$$

Cr(VI) equilibrium removal capacity Q_e (mg g^{-1} dry base) was calculated according to Formula 2-2:

$$Q_e = (C_0 - C_e) \times \frac{V}{m} \tag{2}$$

Removal capacity Q_t (mg g^{-1} dry base) of Cr(VI) at time t was calculated according to Formula 2-3:

$$Q_e = (C_0 - C_t) \times \frac{V}{m} \tag{3}$$

Where C_0 (mg L^{-1}) was the initial concentration of Cr(VI) solution, C_e (mg L^{-1}) was the concentration at equilibrium of Cr(VI) removal, C_t (mg L^{-1}) was the concentration of residual Cr(VI) in the solution at time t, V (mL) was the volume of Cr(VI) solution, and m (g) was the dry weight of adsorbent.

Determination of Cr(VI) concentration
The determination of Cr(VI) concentration was performed according to Huang, et al.[6], by following procedure. First, the potassium dichromate powder was placed in a hot air-drying oven at 65 °C overnight, and 2.829 g was accurately weighed and dissolved with deionized water. The solution was transferred to a 1 L volumetric flask with a constant volume. The solution was used as Cr(VI) mother liquor with a concentration of 1000 mg L^{-1}, and the mother liquor was stored at 4 °C away from light. In this study, Cr(VI) solutions with different initial concentrations were diluted by the above mother liquor according to the dilution ratio.

The concentration of Cr(VI) in the solution was determined by the colorimetric method as follows:
1. Configuration of the chromogenic agent. 2.0 g diphenyl carbazide was dissolved in 90 mL acetone, and 200 μL concentrated sulfuric

acid was added to the solution. Finally, the volume was determined in a 100 mL volumetric flask. After the preparation of the chromogenic agent, the shelf life was 7 d.

2. Cr(VI) standard solution prepared. The standard solution of Cr(VI) was prepared by 50 times the dilution of Cr(VI) mother liquor prepared in 2.2.1, and the concentration was 5 ppm.

3. Cr(VI) standard curve construction. Take 0, 2, 4, 6, 8, 10, 12, and 14 mL standard solution of Cr(VI) in a 50 mL volumetric flask, add 30–40 mL deionized water, then add 1 mL mixture of sulfuric acid and phosphoric acid (1:1), and finally add 2 mL chromogenic agent and constant volume. The reaction was 5 min at room temperature. The reaction system was colorimetric at 540 nm, with deionized water as blank, and the absorbance was recorded. The standard curve was drawn using absorbance and Cr(VI) concentration as horizontal and vertical coordinates.

4. Determination of Cr(VI) concentration: Dilute the solution to a reasonable concentration, determine according to steps (2) and (3), and put it into the standard curve to calculate the concentration of Cr(VI).

Determination of Cr(III) concentration in solution

The determination of Cr(III) concentration in the solution referred to the study of ref. 30. An iCAPQc inductively coupled plasma mass spectrometer (Thermo Electron, the United States) was used to determine the total concentration of chromium in the solution. The concentration of Cr(III) in the solution was obtained by subtracting the concentration of Cr(VI) from the total chromium concentration in the solution.

Cr(VI) removal potentials

The influence of different environmental parameters on the Cr(VI) removal capacities of EW-BC film was investigated. The initial Cr(VI) solution concentration was $100 \, \text{mg L}^{-1}$. The pH values of the Cr(VI) solution were adjusted to 1.0, 2.0, 3.0, 4.0, 5.0, 6.0 and 7.0 with $0.1 \, \text{mol L}^{-1}$ HCl and NaOH solution, respectively. 100 mL Cr(VI) solutions with different pH values were placed in triangular bottles, and EW-BC film was added at the rate of $1 \, \text{g L}^{-1}$ (dry weight). Then the concentration of Cr(VI) remaining in the solution after exposure to EW-BC film was determined by shaking at 180 rpm at 30 °C for 12 h. The removal capacity of BC was calculated.

Next, the influence of different initial Cr(VI) concentrations on BC film removal properties based on the solution's initial pH with maximum clearance was investigated. The concentration of Cr(VI) solution was 100, 200, 300, 400, 500, 600, 700, 800, 900 and $1000 \, \text{mg L}^{-1}$, respectively, and the pH value was adjusted to 1.0. After that, 100 mL of Cr(VI) solutions with different concentrations were placed in triangular bottles, and EW-BC film was added at the rate of $1 \, \text{g L}^{-1}$ (dry weight). Then, the residual Cr(VI) concentration in the solution after exposure to EW-BC film was measured by shaking at 180 rpm at 30 °C for 12 h.

The effect of removal time on Cr(VI) removal properties was investigated. The Cr(VI) concentrations were 300, 500 and $700 \, \text{mg L}^{-1}$, respectively, and the pH was adjusted to 1.0. 100 mL of Cr(VI) solutions with different concentrations were placed in triangular bottles, and the EW-BC film was added at the rate of $1 \, \text{g L}^{-1}$ (dry weight). Then, the remaining concentration of Cr(VI) in the solution was measured every 1 h by shaking at 180 rpm at 30 °C to explore the influence of contact time on the removal effect of BC.

The influence of different coexisting ions on the EW-BC film's Cr(VI) removal property was investigated. $500 \, \text{mg L}^{-1}$ Cr(VI) solution was used as the solvent, and $500 \, \text{mg L}^{-1}$ KCl_2, $CaCl_2$, NaCl, $CuCl_2$, $ZnCl_2$, $NaNO_3$, and Na_2SO_4 solutions were prepared, respectively, and the pH was adjusted to 1.0. 100 mL of Cr(VI) solutions with different co-existing ions were placed in triangular bottles; BC film was added at the rate of $1 \, \text{g L}^{-1}$ (dry weight), and then placed at 30 °C 180 rpm for shaking for 12 h. The concentration of residual Cr(VI) in the solution after exposure to EW-BC film was determined.

Desorption experiment

Desorption of EW-BC film adsorbed Cr(VI) at different pH was evaluated. Adsorption of EW-BC film in Cr(VI) solution with an initial concentration of $500 \, \text{mg L}^{-1}$ at $1 \, \text{g L}^{-1}$ (dry weight) for 24 h. The adsorbed EW-BC film was removed, and the surface moisture was absorbed with filter paper. Then, the EW-BC film was added to deionized water with a pH of 1–8 at $1 \, \text{g L}^{-1}$ (dry weight) dosage and desorbed at 180 rpm at 30 °C for 24 h. The contents of Cr(VI) and Cr(III) in the desorption solution were determined.

Removal kinetics simulation

To further study the removal process of Cr(VI) by EW-BC film, the removal kinetics model was simulated by analyzing the relationship between contact time and removal capacity. This study used the quasi-first-order kinetic and quasi-second-order kinetic equations based on removal equilibrium capacity to simulate removal kinetics.

The pseudo-first-order equation was shown in Eqs. 2–4:

$$\text{Log}(Q_e - Q_t) = \log Q_e - k_1 \times \frac{t}{2.303} \tag{4}$$

In the formula, Q_e (mg g^{-1}) and Q_t (mg g^{-1}) were the removal capacity at Cr(VI) concentration equilibrium of solution and the removal capacity at t (min) time, respectively, and K_1 (min^{-1}) was the first-order kinetic rate constant.

The pseudo-second-order equation was shown in Eqs. 2–5:

$$\frac{t}{Q_t} = \frac{t}{Q_e} + \frac{1}{k_2 \times Q_e^2} \tag{5}$$

In the formula, Q_e (mg g^{-1}) and Q_t (mg g^{-1}) are the removal capacity at removal equilibrium and the removal capacity at t (min) time, respectively, and k_2 $(\text{g·mg}^{-1}\text{·min}^{-1})$ is the second-order kinetic rate constant.

Removal isotherm simulation

The removal isotherm model was used to study the relationship between Cr(VI) equilibrium removal capacity of EW-BC film (Q_e) and Cr(VI) equilibrium concentration of solution (C_e). Langmuir and Freundlich isothermal removal models were used to simulate the equilibrium data.

Langmuir isothermal removal model equation was shown in Eqs. 2–6:

$$\frac{C_e}{Q_e} = \frac{C_e}{Q_m} + \frac{1}{b \times Q_m} \tag{6}$$

In the formula, Q_m was the maximum removal capacity (mg g^{-1}), and b was the Langmuir isothermal constant (L mg^{-1}).

Freundlich isothermal removal model equation was shown in Eqs. 2–7:

$$\ln Q_e = \frac{(1)}{n} \times \ln C_e + \ln k_f \tag{7}$$

In the formula, $\frac{(1)}{n}$ and k_f were the infinite-dimensional constants in the Freundlich model, respectively.

Removal mechanism

The EW-BC film was added to Cr(VI) solution with an initial concentration of $500 \, \text{mg L}^{-1}$ at the rate of $1 \, \text{g L}^{-1}$ (dry weight). After contact at 30 °C for 24 h, the EW-BC film was removed, washed with deionized water three times, and then freeze-dried. BC that did not participate in Cr(VI) removal was used as the control. The freeze-dried BC films before and after adsorption were characterized.

The microstructure of BC before and after adsorption was observed by Scanning electron microscope-energy spectrum analysis (SEM-EDS) (FEI-F50, Zeiss, Germany), and an energy dispersive spectrometer determined the elemental composition.

The samples before and after adsorption were scanned by X-ray photoelectron spectroscopy (XPS) (EscaLab 250Xi, Thermo Fisher, The United States) for full-spectrum and narrow region scanning, and the surface chemical composition was analyzed qualitatively and quantitatively.

Alk-alpha source was used as the radiation source, and the tube voltage and current were 15 kV and 10 mA, respectively.

BC after adsorption was investigated using an X-ray diffractometer (XRD) (D2PHASER, Bruker, the United States) with a Ni-filtered Cu-Kα (α = 0.15418 nm) at a voltage of 40 kV and a filament emission of 40 mA. The freeze-dried BC were scanned radiation in the 2θ range from 5 ° to 60 ° with 0.02 ° (2θ) step and 5 ° min^{-1} scanning rate.

The Fourier Transform Infrared Spectroscopy (FTIR) spectra of BC before and after adsorption were acquired using a Nicolet iS50 FTIR spectrometer (Thermo Nicolet, the United States). For each sample, the spectra were collected over the 4000–500 cm^{-1} range with an accumulation of 64 scans.

The zeta potential on membrane surface was acquired using a zeta potential analyzer for solid (SurPASS 3, Anton Paar, Austria). The BC and EW-BC membrane was trimmed to 1×2 cm, the test temperature was 25 ℃, and the pH range was 1–8.

Statistic analysis

All experiments were conducted in triplicate. Significant differences were determined using GraphPad 8.0 with one-way analysis of variance (ANOVA) by Duncan's test at $p < 0.05$.

Data availability

The datasets generated during and/or analysed during the current study are available from the corresponding author on reasonable request.

Code availability

For access to detailed code implementations, please contact the authors directly.

References

1. Zheng, B., Lin, X., Zhang, X., Wu, D. & Matyjaszewski, K. Emerging Functional Porous Polymeric and Carbonaceous Materials for Environmental Treatment and Energy Storage. *Adv. Funct. Mater.* **30**, 1907006 (2020).
2. Tang, S. et al. Ferrous ion-tartaric acid chelation promoted calcium peroxide fenton-like reactions for simulated organic wastewater treatment. *J. Clean. Prod.* **268**, 122253 (2020).
3. Tian, Y. & Zhou, H. A novel nitrogen-doped porous carbon derived from black liquor for efficient removal of Cr(VI) and tetracycline: Comparison with lignin porous carbon. *J. Clean. Prod.* **333**, 130106 (2022).
4. Zhu, S. et al. Green sustainable and highly efficient hematite nanoparticles modified biochar-clay granular composite for Cr(VI) removal and related mechanism. *J. Clean. Prod.* **276**, 123009 (2020).
5. Alvarez, P. J. J., Chan, C. K., Elimelech, M., Halas, N. J. & Villagrán, D. Emerging opportunities for nanotechnology to enhance water security. *Nat. Nanotechnol.* **13**, 634–641 (2018).
6. Huang, Y., Zeng, Q., Hu, L., Zhong, H. & He, Z. Bioreduction performances and mechanisms of Cr(VI) by *Sporosarcina saromensis* W5, a novel Cr(VI)-reducing facultative anaerobic bacteria. *J. Hazard. Mater.* **413**, 125411 (2021).
7. Pradhan, D., Sukla, L. B., Sawyer, M. & Rahman, P. K. Recent bioreduction of hexavalent chromium in wastewater treatment: A review. *J. Ind. Eng. Chem* **55**, 1–20 (2017).
8. Pakade, V. E., Tavengwab, N. T. & Madikizelac, L. M. Recent advances in hexavalent chromium removal from aqueous solutions by adsorptive methods. *RSC Adv* **9**, 26142–26164 (2019).
9. Sharma, A. K. et al. Reductive-co-precipitated cellulose immobilized zerovalent iron nanoparticles in ionic liquid/water for Cr(VI) adsorption. *Cellulose* **25**, 5259–5275 (2018).
10. Wu, J., Wang, X. B. & Zeng, R. J. Reactivity enhancement of iron sulfide nanoparticles stabilized by sodium alginate: Taking Cr (VI.) removal as an example. *J. Hazard. Mate.* **333**, 275–284 (2017).
11. Zhou, L. et al. Investigation of the adsorption-reduction mechanisms of hexavalent chromium by ramie biochars of different pyrolytic temperatures. *Bioresource Technol* **218**, 351–359 (2016).
12. Dong, Z. & Zhao, L. Covalently bonded ionic liquid onto cellulose for fast adsorption and efficient separation of Cr(VI): Batch, column and mechanism investigation. *Carbohyd. Polym.* **189**, 190–197 (2018).
13. Lv, X., Xu, J., Jiang, G. & Xu, X. Removal of chromium(VI) from wastewater by nanoscale zero-valent iron particles supported on multiwalled carbon nanotubes. *Chemosphere* **85**, 1204–1209 (2011).
14. Liu, C. et al. Direct/alternating current electrochemical method for removing and recovering heavy metal from water using graphene oxide electrode. *ACS Nano.* **13**, 6431–6437 (2019).
15. Zhang, Z. et al. One-pot preparation of P(TA-TEPA)-PAM-RGO ternary composite for high efficient Cr(VI) removal from aqueous solution. *Chem. Eng. J.* **343**, 207–216 (2018).
16. Shao, Z. et al. Ion exchange collaborating coordination substitution: More efficient Cr(VI) removal performance of a water-stable Cu^{II}-MOF material. *J. Hazard. Mater.* **378**, 120719 (2019).
17. Uliana, A. A. et al. Ion-capture electrodialysis using multifunctional adsorptive membranes. *Science* **372**, 296–299 (2021).
18. Aziz, F. F. A. et al. CuO improved energy band of AgO/fibrous SiO2-ZrO2 for optimized simultaneous photocatalytic redox of chromium (VI) and p-cresol using response surface methodology. *Environ. Res.* **220**, 115151 (2023).
19. Nguyen, T. A. H. et al. Applicability of agricultural waste and by-products for adsorptive removal of heavy metals from wastewater. *Bioresource Technol* **148**, 574–585 (2013).
20. Wu, Y. et al. Multi-functional magnetic water purifier for disinfection and removal of dyes and metal ions with superior reusability. *J. Hazard. Mater* **347**, 160–167 (2018).
21. Jiang, Z., Ho, S.-H., Wang, X., Li, Y. & Wang, C. Application of biodegradable cellulose-based biomass materials in wastewater treatment. *Environ. pollut.* **290**, 118087 (2021).
22. Wu, Z., Liang, H., Chen, L., Hu, B. & Yu, S. Bacterial cellulose: A robust platform for design of three dimensional carbon-based functional nanomaterials. *Acc. Chem. Res.* **49**, 96–105 (2016).
23. Hu, W., Chen, S., Yang, J., Li, Z. & Wang, H. Functionalized bacterial cellulose derivatives and nanocomposites. *Carbohyd. Polym.* **101**, 1043–1060 (2014).
24. Su, K. et al. One-pot green synthesis of poly(hexamethylenediamine-tannic acid)-bacterial cellulose composite for the reduction, immobilization, and recovery of Cr(VI). *J. Environ. Chem. Eng.* **10**, 107026 (2022).
25. Lu, M., Xu, Y., Guan, X. & Wei, D. Preliminary research on Cr(VI) removal by bacterial cellulose. *J. Wuhan Univ. Technol* **27**, 572–575 (2012).
26. Santos-Buelga, C., González-Paramás, A. M., Oludemi, T., Ayuda-Durán, B. & González-Manzano, S. Plant phenolics as functional food ingredients. *Adv. Food. Nutr. Res.* **90**, 183–257 (2019).
27. Jiang, X. et al. Reductive transformation of Cr(VI) in contaminated soil by polyphenols: The role of gallic and tannic acid. *Ecotox. environ. safe.* **255**, 114807 (2023).
28. Chand, R. et al. Grape waste as a biosorbent for removing Cr(VI) from aqueous solution. *J. Hazard. Mater.* **163**, 245–250 (2009).
29. Li, Z. et al. Green and efficient in-situ biosynthesis of antioxidant and antibacterial bacterial cellulose using wine pomace. *Int. J. Biol. Macromol.* **193**, 2183–2191 (2021).
30. Shi, X., Qiao, Y., An, X., Tian, Y. & Zhou, H. High-capacity adsorption of Cr(VI) by lignin-based composite: Characterization, performance and mechanism. *Int. J. Biol. Macromol.* **159**, 839–849 (2020).
31. Park, D., Yun, Y., Lee, H. W. & Park, J. M. Advanced kinetic model of the Cr(VI) removal by biomaterials at various pHs and temperatures. *Bioresource Technol* **99**, 1141–1147 (2008).

32. Nakano, Y., Takeshita, K. & Tsutsumi, T. Adsorption mechanism of hexavalent chromium by redox within condensed-tannin gel. *Water Res* **35**, 496–500 (2001).

33. Dong, L. et al. Hierarchical polydopamine coated cellulose nanocrystal microstructures as efficient nanoadsorbents for removal of Cr(VI) ions. *Cellulose* **26**, 6401–6414 (2019).

34. Peng, X. et al. Adsorption behavior of hexavalent chromium in aqueous solution by polyvinylimidazole modified cellulose. *Int. J. Biol. Macromol.* **155**, 1184–1193 (2020).

35. Omer, A. M., El-Monaem, E. M. A. & Eltaweil, A. S. Novel reusable amine-functionalized cellulose acetate beads impregnated aminated graphene oxide for adsorptive removal of hexavalent chromium ions. *Int. J. Biol. Macromol.* **208**, 925–934 (2022).

36. Song, X. et al. Enhanced biostimulation coupled with a dynamic groundwater recirculation system for Cr(VI) removal from groundwater: A field-scale study. *Sci. Total Environ.* **772**, 145495 (2021).

37. Aksu, Z. Equilibrium and kinetic modelling of cadmium(II) biosorption by C. vulgaris in a batch system: effect of temperature. *Sep. purif. technol.* **21**, 285–294 (2001).

38. Shao, Y. et al. Polypyrrole/bacterial cellulose nanofiber composites for hexavalent chromium removal. *Cellulose* **28**, 2229–224 (2021).

39. Yang, S., Liao, Y., Karthikeyan, K. G. & Pan, X. J. Mesoporous cellulose-chitosan composite hydrogel fabricated via the co-dissolution-regeneration process as biosorbent of heavy metals. *Environ. Pollut.* **286**, 117324 (2021).

40. Jahan, K., Kumar, N. & Verma, V. Bacterial cellulose/PANi mat for Cr(VI) removal at acidic pH. *J. Appl. Polym. Sci.* **138**, 51309 (2021).

41. Dong, L. et al. Effect of coexisting ions on Cr(VI) adsorption onto surfactant modified Auricularia auricula spent substrate in aqueous solution. *Ecotox. Environ. Safe* **166**, 390–400 (2018).

42. Apak, R., Guclu, K., Ozyurek, M., Bektasoglu, B. & Bener, M. Cupric ion reducing antioxidant capacity assay for food antioxidants: vitamins, polyphenolics, and flavonoids in food extracts. *Method. Mol. Biol.* **477**, 163–193 (2008).

43. Cho, D. et al. Adsorption of nitrate and Cr(VI) by cationic polymer-modified granular activated carbon. *Chem. Eng. J.* **175**, 298–305 (2011).

44. Simonin, J. On the comparison of pseudo-first order and pseudo-second order rate laws in the modeling of adsorption kinetics. *Chem. Eng. J.* **300**, 254–263 (2016).

45. Jung, K. W., Lee, S. Y. & Lee, Y. J. Facile one-pot hydrothermal synthesis of cubic spinel_type manganese ferrite/biochar composites for environmental remediation of heavy metals from aqueous solutions. *Bioresource Technol* **234**, 1–9 (2018).

46. Yu, W., Zhou, X. & Li, C. Application of first-order kinetics modeling to reveal the nature of starch digestion characteristics. *Food. funct.* **12**, 6652–6663 (2021).

47. Lagergren, S. About the theory of so-called adsorption of soluble substances. *J. Handlingar*, 1–39 (1898).

48. Blanchard, G., Maunaye, M. & Martin, G. Removal of heavy metals from waters by means of natural zeolites. *Water Res* **18**, 1501–1507 (1984).

49. Moharram, M. A. & Mahmoud, O. M. FTIR spectroscopic study of the effect of microwave heating on the transformation of cellulose I into cellulose II during mercerization. *J. Appl. Polym. Sci.* **107**, 30–36 (2008).

50. Castro, C. et al. Structural characterization of bacterial cellulose produced by *Gluconacetobacter swingsii* sp. from Colombian agroindustrial wastes. *Carbohyd. Polym.* **84** (2010).

51. Chen, J. et al. In situ preparation of bacterial cellulose with antimicrobial properties from bioconversion of mulberry leaves. *Carbohyd. Polym.* **220**, 170–175 (2019).

52. Wada, M., Heux, L. & Sugiyama, J. Polymorphism of Cellulose I Family: Reinvestigation of Cellulose IVI. *Biomacromolecules* **5**, 1385–1391 (2004).

53. Jin, W., Lee, I. K. & Kompch, A. Chemical vapor synthesis and characterization of chromium doped zinc oxide nanoparticles. *J. Eur. Ceram. Soc* **27**, 4333–4337 (2008).

54. Wang, P., Ji, W., Li, M., Zhang, G. & Wang, J. $Bi_{25}VO_{40}$ microcube with step surface for visible light photocatalytic reduction of Cr(VI): Enhanced activity and ultrasound assisted regeneration. *Ultrason. Sonochem.* **38**, 289–297 (2017).

55. Almontasser, A. & Parveen, A. Preparation and characterization of chromium oxide nanoparticles. *AIP Conf. Proc.* **2220**, 020010 (2020).

56. Yasmeen, G. et al. Green synthesis of Cr_2O_3 nanoparticles by cassia fistula, their electrochemical and antibacterial potential. *Arab. Chem.* **16**, 104912 (2023).

57. Liu, K., Shi, Z. & Zhou, S. Reduction of hexavalent chromium using epigallocatechin gallate in aqueous solutions: kinetics and mechanism. *RSC Adv* **6**, 67196–67203 (2016).

58. Chen, Z., Zhao, Y. & Li, Q. Characteristics and kinetics of hexavalent chromium reduction by gallic acid in aqueous solutions. *Water Sci. Technol.* **71**, 1694–1700 (2015).

Acknowledgements

Author contributions

Zhi-yu Li: Data curation, Software, Formal analysis, Investigation, Writing – original draft, preparation. Jia-jia Dong: Methodology, Software. Fidelis Azi: Methodology, Software. Xue Feng: Conceptualization. Zhi-wen Ge: Supervision. Sha Yang: Methodology. Yu-xia Sun: Visualization, Supervision. Xue-qiang Guan: Supervision, Project administration. Ming-sheng Dong: Project administration, Writing - review & editing. All authors read and approved the final manuscript.

Competing interests

The authors declare no competing interests.

Additional information